NASA Technical Memorandum 100132

Turbulence Modeling and Surface Heat Transfer in a Stagnation Flow Region

Chi R. Wang and Frederick C. Yeh
Lewis Research Center
Cleveland, Ohio

Prepared for the
1987 Winter Annual Meeting of the
American Society of Mechanical Engineers
Boston, Massachusetts, December 13-18, 1987

NASA

TURBULENCE MODELING AND SURFACE HEAT TRANSFER IN A STAGNATION FLOW REGION

Chi R. Wang and Frederick C. Yeh
National Aeronautics and Space Administration
Lewis Research Center
Cleveland, Ohio 44135

E-3682

ABSTRACT

Analysis for the turbulent flow field and the effect of freestream turbulence on the surface heat transfer rate of a stagnation flow is presented. The emphasis is on the modeling of turbulence and its augmentation of surface heat transfer rate. The flow field considered is the region near the forward stagnation point of a circular cylinder in a uniform turbulent mean flow. The freestream is steady and incompressible with a Reynolds number of the order of 10^5 and turbulence intensity of <5 percent. The flow field is divided into three regions: (1) a uniform freestream region where the turbulence is homogeneous and isotropic; (2) an external inviscid flow region where the turbulence is distorted by the variation of the mean velocity; and (3) an anisotropic turbulent boundary layer flow region. The turbulence modeling techniques are the k-ε two-equation model in the external flow and the time-averaged turbulence transport equation in the boundary layer. The turbulence double correlations, the mean velocity, and the mean temperature within the boundary layer are solved numerically from the transport equations. The surface heat transfer rate is calculated as functions of the freestream turbulence longitudinal microlength scale, turbulence intensity, and Reynolds number.

NOMENCLATURE

$A_{\xi i}, A_{\eta i}$	coefficients of Eqs. (A1) and (A2), i = 1 to 5 mean velocity parameter
B	coefficients of Eq. (A5), i = 1 to 4
c_i	empirical constants, i = 1 to 5
c_μ	empirical constant
D	cylinder diameter
E	dimensionless turbulence dissipation rate
F	dimensionless mean flow streamwise velocity
f_i	parametrical functions of φ_0, i = 1 to 3
G	flow variable of Eqs. (A1) and (A2)
H	dimensionless mean temperature
K	dimensionless turbulence kinetic energy
k	turbulence kinetic energy
ℓ	spatial distance
Nu	Nusselt number
Pr	Prandtl number, 0.7
R	sum of dimensionless Reynolds normal stresses, $R_X + R_Y + R_Z$
Re	Reynolds number
R_X	dimensionless Reynolds normal stress along x-direction
R_y	dimensionless Reynolds normal stress along y-direction
R_Z	dimensionless Reynolds normal stress along z-direction
S	dimensionless Reynolds shear stress
T	mean temperature
Tu	freestream turbulence intensity
t	temperature fluctuation
U,V	mean flow velocity components
V_t	transformed velocity of V, Eq. (11)
u,v,w	velocity fluctuations

x,y,z	physical coordinate system
δ	stagnation point laminar boundary layer thickness
ϵ	turbulence dissipation rate
η	transformed coordinate along y-direction
θ	dimensionless turbulence correlation,
Λ	turbulence modeling length scale
λ	turbulence longitudinal microlength scale
ν	kinematic viscosity
ξ	transformed coordinate along x-direction
ρ	density
φ	azimuth angle
-	time-averaged quantity

Subscripts:

0	condition near stagnation point ($\varphi = 0.04^\circ$)
1	condition at location 1
2	condition at location 2 of boundary layer edge
3	condition at location 3 of boundary layer edge
e	external or boundary layer edge condition
0,e	boundary layer edge condition at initial station
F	freestream condition
m	grid point along ξ or η direction
w	surface condition

INTRODUCTION

The momentum and thermal flow fields near the forward stagnation point of a circular cylinder in turbulent flow have been the focus of considerable study. When the turbulence intensity was 3 to 5 percent, existing experiments have shown that the local Nusselt number can increase by about 75 percent as compared with laminar flow conditions. With the current emphasis on high turbine inlet temperature, it has become even more important to understand the effect of turbulence on the surface heat transfer, particularly in the leading edge stagnation region. To estimate this surface heat transfer rate, correlations derived from experimental data may be used. Detailed experimental data can be found in the paper by Lowery and Vachon (1). An alternative is to rely on theoretical analysis to predict the surface heat transfer rate. The objective of the present study is to develope an analysis which predicts the effect of turbulence on surface heat transfer rate.

Existing boundary layer flow analyses (2,3) indicated a large effect of turbulence on the stagnation point heat transfer rate. Other studies (4 to 8) showed that turbulence amplification because of vortex stretching can also influence the thin boundary layer, and therefore the surface heat transfer rate. Hijikata et al. (9) performed a theoretical and experimental study of the stagnation point anisotropic turbulence. This analysis showed that the turbulence length scale also affects the surface heat transfer rate. Traci and Wilcox (10) analytically studied the turbulence effect on the stagnation point flow field. The mean velocity gradients within the inviscid flow were found to be important in analyzing the stagnation point heat transfer. A difficulty in this type of analysis is obtaining a proper match of the boundary conditions between the different flow regions. Strahle (11) tried to resolve the turbulence matching conditions. Analytical relations between the turbulence properties at the stagnation point and in the freestream were found. In a previous study (12) Wang proposed a theoretical boundary layer flow analysis and numerical computational procedure to investigate the turbulence, momentum, and thermal fields within the stagnation flow region. The numerical calculation showed that rapid amplification of the Reynolds normal stress along the boundary layer edge was required to predict approximately the surface heat transfer rate as reported in existing experiments.

Based on the experimental results and analytical methods of the existing studies (1, 10 to 12), it is possible to pursue a detailed theoretical and numerical analysis of the forward stagnation flow field of a circular cylinder in a turbulent freestream. Reported herein is such an analysis which predicts the surface heat transfer rate as functions of the freestream turbulence longitudinal microlength scale, turbulence intensity, and Reynolds number. The emphasis is on the modeling of turbulence and its augmentation of the surface heat transfer rate.

The flow field is divided into three regions: (1) a region away from the cylinder where the mean velocity is uniform and the turbulence is assumed to be homogeneous and isotropic, (2) an external inviscid flow region which has a constant rate of mean velocity variation and the mean velocity distorts the turbulence, and (3) a boundary layer region over the cylinder surface. For turbulence modeling, the k-ϵ two-equation modeling and the time-averaged turbulence transport equation are used respectively in Flow Regions 2 and 3. These turbulence modeling equations and the mean flow conservation equations are used to formulate the theoretical analysis. The turbulence double correlations, the mean velocity, and the mean temperature within the boundary layer region are solved numerically from the turbulence transport equations and mean flow conservation equations. The solution is obtained by matching the turbulence kinetic energy along the boundary between the flow regions. These analytical results are compared with the measurements from the existing experiments.

ANALYTICAL FORMULATION OF FLOW REGIONS

The flow region of interest is around the forward stagnation point of a circular cylinder in a turbulent freestream. Figure 1 schematically represents the flow field. The diameter of the cylinder is D and its axis is perpendicular to the freestream mean velocity V_F. The freestream Reynolds number is defined as $Re = V_F D/\nu$, where ν is the kinematic viscosity. The velocity fluctuation in the freestream is v_F and the freestream turbulence intensity is defined as $Tu = \sqrt{\overline{v_F^2}}/V_F$. The freestream turbulence longitudinal microlength scale is denoted by λ_F. The cylinder

is assumed to have a constant surface temperature T_W. The freestream has a mean temperature T_F.

The stagnation point is taken as the coordinate-system origin with x and y coordinates parallel to and normal to the cylinder surface and z-coordinate parallel to the cylinder axis. The mean flow field is assumed steady, incompressible, and two-dimensional. The mean velocity components are U and V along the x- and y coordinates. The turbulence is three-dimensional. The velocity fluctuations are denoted by u, v, and w along the x-, y-, and z-directions. The governing equations of the mean flow and turbulence are derived for each flow region. Following the laminar flow analysis, the relations

$$\xi(x) = \int_0^x \frac{U_e}{\nu}\, dx, \quad \text{and} \quad \eta(x,y) = \frac{\frac{U_e y}{\nu}}{(2\xi)^{0.5}} \qquad (1)$$

are used for coordinate transformation. The analytical formulation, together with the assumptions and the boundary conditions, is described here.

Region 1

This flow region is far away from the cylinder. The flow is turbulent and its mean velocity is uniform. The properties of the mean flow and its turbulence are not influenced by the existence of the cylinder. Appropriate conditions of the turbulence kinetic energy k, and the turbulence dissipation rate ε, are required to characterize the turbulence. The turbulence is assumed to be homogeneous and isotropic. The freestream turbulence kinetic energy and the turbulence dissipation rate are given in Ref. 13 as

$$k_F = \frac{3\overline{v_F^2}}{2}, \quad \text{and} \quad \varepsilon_F = \frac{30\nu\overline{v_F^2}}{\lambda_F^2} \qquad (2)$$

The turbulence longitudinal microlength scale is determined from the two point turbulence correlations (13). The longitudinal two point turbulence correlation g, the spacial distance ℓ, and the turbulence longitudinal microlength scale are related by the following relations for small ℓ.

$$g(\ell) = 1 - \frac{\ell^2}{\lambda_F^2} \qquad (3)$$

Region 2

In this region, the mean velocity is disturbed by the cylinder. The mean velocity variation distorts the turbulence. It is assumed that the turbulence does not influence the mean velocity. Thus, the mean velocity is represented with the two-dimensional inviscid flow solution near the stagnation point. The mean velocity components are

$$U = ax \quad \text{and} \quad V = -ay \qquad (4)$$

with $a = 4V_F/D$. The turbulence kinetic energy variation along the stagnation point streamline is of interest in this study. The turbulence is modeled with the $k-\varepsilon$ two-equation turbulence modeling (14).

Introducing Eqs. (1) and (4) into the standard k and ε equations, neglecting the diffusion terms in the x-direction and seeking the following forms of solutions:

$$k = \nu a K(\eta) \quad \text{and} \quad \varepsilon = \nu a^2 E(\nu) \qquad (5)$$

the k and ε equations become

$$\eta \frac{dK}{d\eta} = -4c_\mu \frac{K^2}{E} + E - \frac{d}{d\eta}\left(c_\mu \frac{K^2}{c_3 E}\frac{dK}{d\eta}\right) \qquad (6)$$

$$\eta \frac{dE}{d\eta} = -4c_1 c_\mu K + c_2 \frac{E^2}{k} - \frac{d}{d\eta}\left(c_\mu \frac{K^2}{c_4 E}\frac{dE}{d\eta}\right) \qquad (7)$$

along the stagnation point streamline. The empirical constants are $c_1 = 1.44$, $c_2 = 1.92$ $c_3 = 1.00$, $c_4 = 1.30$, and $c_\mu = 0.09$.

Equations (6) and (7) are solved for the turbulence properties K and E in the interval $\eta_1 \geq \eta \geq \eta_2$, where η_1 is the boundary between Flow Regions 1 and 2, and η_2 is the boundary between Flow Regions 2 and 3.

The boundary conditions are defined in the following:

1. At $\eta = \eta_1$,

$$K = K_1 = \frac{k_F}{\nu a}, \quad \text{and} \quad E = E_1 = \frac{\varepsilon_F}{\nu a^2} \qquad (8)$$

where k_F and ε_F are previously determined by Eq. (2).

2. Neglecting the diffusion term in Eq. (7) at η_1, this equation gives the following additional boundary condition at $\eta = \eta_1$.

$$\frac{dE}{d\eta} = \frac{1}{\eta_1}\left(c_2 \frac{E_1^2}{K_1} - 4c_1 c_\mu K_1\right) \qquad (9)$$

3. It is also assumed (10) that

$$\frac{dK}{d\eta} = 0 \quad \text{at} \quad \eta = \eta_2 \qquad (10)$$

The finite difference method is used to solve the above boundary value problem. A summary of the computational procedure is given in Appendix A. The relation $\eta_1 = V_F/(a\nu)^{0.5}$ is found from Eqs. (1) and (4), and η_2 is resolved in the process of the numerical calculation. The computational results of the turbulence properties K and E at $\eta = \eta_2$ are used to analyze the boundary layer flow region.

Region 3

A steady, two-dimensional, and incompressible turbulent boundary layer is assumed in the boundary layer region. The mean flow properties are described by the boundary layer continuity, momentum, and enthalpy equations. The momentum and enthalpy equations contain turbulence double correlations, $\overline{uv}$ and $\overline{vt}$. A method to model the turbulence double correlations within a turbulent flow was developed by Donaldson et al. (15 and 16). This method is used to formulate a theoretical analysis of the turbulence in this flow region. The time-averaged turbulence transport equations are derived following the theory in

Ref. 15. Assumptions are made for the turbulence closure relations and a modeling length scale Λ. Details of the theoretical formulation and assumptions can be found in Refs. 15 to 17.

The mean flow velocity $U_e = ax$ is assumed along the boundary layer edge between regions 2 and 3. The mean flow properties and turbulence double correlations are also nondimensionalized as

$$F = \frac{U}{U_e} \qquad H = \frac{T}{T_e}$$

$$R_x = \frac{\overline{u^2}}{U_e^2}, \quad R_y = \frac{\overline{v^2}}{U_e^2}, \quad R_z = \frac{\overline{w^2}}{U_e^2}$$

$$S = -\frac{\overline{uv}}{U_e^2}, \quad \theta = -\frac{\overline{vt}}{U_e T_e}$$

Introducing the above dimensionless variables and Eq. (1) into the mean flow and turbulence transport equations results in the following forms of the flow field governing equations:

Continuity equation:

$$2\xi \frac{\partial F}{\partial \xi} + \frac{\partial V_t}{\partial \eta} + F = 0 \tag{11}$$

where $V_t = \frac{2\xi\nu F}{U_e}\frac{\partial \eta}{\partial x} + (2\xi)^{0.5}\frac{V}{U_e}$

Momentum equation:

$$2\xi F \frac{\partial F}{\partial \xi} + V_t \frac{\partial F}{\partial \eta} = \frac{2\xi(1 - F^2)}{U_e}\frac{\partial U_e}{\partial \xi} + \frac{\partial^2 F}{\partial \eta^2} + (2\xi)^{0.5}\frac{\partial S}{\partial \eta} \tag{12}$$

Enthalpy equation:

$$2\xi F \frac{\partial H}{\partial \xi} + V_t \frac{\partial H}{\partial \eta} = -\frac{2\xi F H}{T_e}\frac{\partial T_e}{\partial \xi} + \frac{1}{Pr}\frac{\partial^2 H}{\partial \eta^2} + (2\xi)^{0.5}\frac{\partial \theta}{\partial \eta} \tag{13}$$

Turbulence equations:

$$2\xi F \frac{\partial R_x}{\partial \xi} + V_t \frac{\partial R_x}{\partial \eta} = -2\xi \frac{4R_x F}{U_e}\frac{\partial U_e}{\partial \xi} + \frac{U_e}{\nu}\frac{\partial}{\partial \eta}\left(\Lambda R^{0.5}\frac{\partial R_x}{\partial \eta}\right) + \frac{\partial^2 R_x}{\partial \eta^2} + 2S(2\xi)^{0.5}\frac{\partial F}{\partial \eta} + 2\xi\frac{(R - 3R_x)}{3}\frac{\nu R^{0.5}}{\Lambda U_e} + 2\xi R_x\left(-2\frac{\partial F}{\partial \xi} - \frac{2\nu}{U_e}\frac{\partial F}{\partial \eta}\frac{\partial \eta}{\partial x} - \frac{2\nu^2}{U_e^2\Lambda^2}\right) \tag{14}$$

$$2\xi F \frac{\partial R_y}{\partial \xi} + V_t \frac{\partial R_y}{\partial \eta} = 5\frac{U_e}{\nu}\frac{\partial}{\partial \eta}\left(\Lambda R^{0.5}\frac{\partial R_y}{\partial \eta}\right) + \frac{\partial^2 R_y}{\partial \eta^2} + 2\xi\frac{\nu R^{0.5}}{\Lambda U_e}\frac{(R - 3R_y)}{3} + 2\xi R_y\left(2\frac{\partial F}{\partial \xi} + \frac{2\nu}{U_e}\frac{\partial F}{\partial \eta}\frac{\partial \eta}{\partial x} - \frac{2\nu^2}{U_e^2\Lambda^2}\right) \tag{15}$$

$$2\xi F \frac{\partial R_z}{\partial \xi} + V_t \frac{\partial R_z}{\partial \eta} = -2\xi \frac{2R_z F}{U_e}\frac{\partial U_e}{\partial \xi} + \frac{U_e}{\nu}\frac{\partial}{\partial \eta}\left(\Lambda R^{0.5}\frac{\partial R_z}{\partial \eta}\right) + \frac{\partial^2 R_z}{\partial \eta} + 2\xi\frac{\nu R^{0.5}}{\Lambda U_e}\frac{(R - 3R_z)}{3} - 2\xi R_z\frac{2\nu^2}{U_e^2\Lambda^2} \tag{16}$$

$$2\xi F \frac{\partial S}{\partial \xi} + V_t \frac{\partial S}{\partial \eta} = -2\xi\frac{2FS}{U_e}\frac{\partial U_e}{\partial \xi} + 3\frac{U_e}{\nu}\frac{\partial}{\partial \eta}\left(\Lambda R^{0.5}\frac{\partial S}{\partial \eta}\right) + \frac{\partial^2 S}{\partial \eta^2} + (2\xi)^{0.5} R_y\frac{\partial F}{\partial \eta} + 2\xi S\left(-\frac{\nu R^{0.5}}{U_e\Lambda} - \frac{2\nu^2}{U_e^2\Lambda^2}\right) \tag{17}$$

and

$$2\xi F \frac{\partial \theta}{\partial \xi} + V_t \frac{\partial \theta}{\partial \eta} = -2\xi\frac{F\theta}{T_e}\frac{\partial T_e}{\partial \xi} + 3\frac{U_e}{\nu}\frac{\partial}{\partial \eta}\left(\Lambda R^{0.5}\frac{\partial \theta}{\partial \eta}\right) + \frac{\partial^2 \theta}{\partial \eta^2} + (2\xi)^{0.5} R_y\frac{\partial H}{\partial \eta} + 2\xi\theta\left(\frac{\partial F}{\partial \xi} + \frac{\nu}{U_e}\frac{\partial F}{\partial \eta}\frac{\partial \eta}{\partial x} - \frac{\nu R^{0.5}}{U_e\Lambda} - \frac{2\nu^2}{U_e^2\Lambda^2}\right) \tag{18}$$

where $R = R_x + R_y + R_z$.

The length scale Λ is required in the formulation of the above turbulence equations. This length scale distribution within the boundary layer is also assumed similar to the mixing length profile of a flat plate turbulent boundary layer. Within a small distance from the surface, the length scale is assumed to vary linearly as function of the normal distance from the surface. Away from the surface, the length scale remains constant. This length scale distribution is shown in Fig. 2. The pivot point, y_p, is equal to 10 percent of the theoretical laminar stagnation point boundary layer thickness δ. At the boundary layer edge, the length scale Λ_e is related to the freestream turbulence intensity by $\Lambda_e = (0.25 - 3Tu)\delta$.

To solve the above governing equations for the mean flow and turbulence properties, the initial and boundary conditions are derived analytically as follows:

Initial conditions. The initial profiles of the mean flow and the turbulence correlations within the boundary layer at $\varphi = \varphi_0$ are determined from Eqs. (11) to (18). The following assumptions are made:

1. At $\eta 2$,

$$\frac{\partial F}{\partial \eta} = 0, \quad \frac{\partial H}{\partial \eta} = 0, \quad \frac{\partial R_x}{\partial \eta} = 0, \quad \frac{\partial R_y}{\partial \eta} = 0, \quad \frac{\partial R_z}{\partial \eta} = 0,$$

$$\frac{\partial S}{\partial \eta} = 0, \quad \text{and} \quad \frac{\partial \theta}{\partial \eta} = 0.$$

In addition, the conditions of

$$F = 1, \quad H = 1, \quad S = c_5(R_x R_y)^{0.5}, \quad \text{and} \quad \theta = 0$$

are also imposed at η_2. An empirical constant, $c_5 = 0.001$ is used in this study.

2. The Reynolds normal stress components $\overline{u^2}$ and $\overline{v^2}$ are assumed to be independent of φ in the vicinity of the stagnation point. Therefore, at φ_o,

$$\frac{\partial R_x}{\partial \xi} = R_x\left(\frac{-2}{R_e \varphi_o^2}\right) \tag{19}$$

and

$$\frac{\partial R_y}{\partial \xi} = R_y\left(\frac{-2}{R_e \varphi_o^2}\right) \tag{20}$$

Similarly,

$$\frac{\partial R_z}{\partial \xi} = R_z f_1(\varphi_o) \tag{21}$$

$$\frac{\partial S}{\partial \xi} = S f_2(\varphi_o) \tag{22}$$

and

$$\frac{\partial \theta}{\partial \xi} = \theta f_3(\varphi_o) \tag{23}$$

are also assumed at φ_o.

3. The mean flow is symmetric about $\varphi = 0$ plane. In order to facilitate the analysis, these mean flow conditions are also assumed to be true at very small distances away from the stagnation point. Therefore, $\partial F/\partial \xi = 0$ and $\partial H/\partial \xi = 0$ are imposed along the η direction at φ_o location.

4. The conditions $F = 0$, $H = T_w/T_e$, $R_x = 0$, $R_y = 0$, $R_z = 0$, $S = 0$, and $\theta = 0$ are also imposed at the cylinder surface.

Applying the above assumptions to the turbulence transport equations, the following relations are found at (φ_o, η_2) location.

$$R_{x,o,e} = \frac{\dfrac{\nu R_{o,e}^{1.5}}{3U_{o,e}\Lambda_e}}{\dfrac{-2}{Re\varphi_o^2} + \dfrac{4(dU/d\xi)_{o,e}}{U_{o,e}} + \dfrac{\nu R_{o,e}^{0.5}}{U_{o,e}\Lambda_e} + \dfrac{2\nu^2}{U_{o,e}^2\Lambda_e^2}} \tag{24}$$

$$R_{y,o,e} = \frac{\dfrac{\nu R_{o,e}^{1.5}}{3U_{o,e}\Lambda_e}}{\dfrac{-2}{Re\varphi_o^2} + \dfrac{\nu R_{o,e}^{0.5}}{U_{o,e}\Lambda_e} + \dfrac{2\nu^2}{U_{o,e}^2\Lambda_e^2}} \tag{25}$$

$$f_1(\varphi_o) = -\frac{2(dU/d\xi)_{o,e}}{U_{o,e}} + \frac{\nu R_{o,e}^{1.5}}{3U_{o,e}R_{z,o,e}\Lambda_e} \tag{26}$$

and

$$f_2(\varphi_o) = -\frac{2(dU/d\xi)_{o,e}}{U_{o,e}} - \frac{\nu R_{o,e}^{0.5}}{U_{o,e}\Lambda_e} - \frac{2\nu^2}{U_{o,e}^2\Lambda_e^2} \tag{27}$$

where $R_{o,e} = 2\nu aK_2/U_{o,e}^2$. Since $\theta = 0$ is imposed at η_2, $d\theta/d\xi = 0$ occurs at the boundary layer edge. This zero gradient condition is also used for the boundary layer calculation at φ_o. It follows from the assumption, Eq. (23), that

$$f_3(\varphi_o) = 0 \tag{28}$$

With the aid of $f_1(\varphi_o)$, $f_2(\varphi_o)$, and $f_3(\varphi_o)$, assumption 2 defines the mean flow streamwise turbulence gradient terms. Substituting Eqs. (19) to (23) into Eqs. (11) to (18) results in a set of ordinary differential equations with the boundary conditions specified at the surface ($\eta = 0$) and at η_2. These equations are solved numerically for the boundary layer flow property profiles at $\varphi_o = 0.04^\circ$ in order to avoid the singularity at the stagnation point, $\varphi = 0.0^\circ$. These property profiles are the initial conditions for the downstream boundary layer flow field analysis.

Boundary conditions. The turbulence double correlations along the boundary layer edge are also required to analyze the flow field. Turbulence kinetic energy and dissipation rate gradients in the normal direction are assumed to be zero ($\partial k/\partial y = 0$, $\partial \varepsilon/\partial y = 0$) at the boundary layer edge. The turbulence kinetic energy along the streamwise direction is determined by using the k-ε two-equation turbulence modeling. The turbulence kinetic energy is then substituted into the Reynolds stress equations to determine the turbulence double correlations along the boundary layer edge.

Introducing Eqs. (1) and (4) into the k-ε equations and seeking the following forms of solutions:

$$k = \nu aK(\xi) \quad \text{and} \quad \varepsilon = \nu a^2 E(\xi) \tag{29}$$

the k and ε turbulence modeling equations become

$$2\xi \frac{dK}{d\xi} = 4c_\mu \frac{K^2}{E} - E + 2\xi \frac{d}{d\xi}\left(c_\mu \frac{K^2}{c_3 E}\frac{dK}{d\xi}\right) \tag{30}$$

$$2\xi \frac{dE}{d\xi} = 4c_1 c_\mu K - c_2 \frac{E^2}{K} + 2\xi \frac{d}{d\xi}\left(c_\mu \frac{K^2}{c_4 E}\frac{dE}{d\xi}\right) \tag{31}$$

From Eqs. (5) to (10) the initial conditions:

$$K = K_2 \quad \text{and} \quad E = E_2 \tag{32}$$

are defined at (ξ_2, η_2).

With the assumption that the gradients $\partial R_x/\partial n$, $\partial R_y/\partial n$, and $\partial R_z/\partial n$ vanish at the boundary layer edge, Eqs. (16) to (18) give the following relations among the mean velocity, the Reynolds normal stresses, and their mean flow streamwise gradients;

$$\frac{dR_{x,e}}{d\xi} = -\frac{4R_{x,e}}{U_e}\frac{dU_e}{d\xi} + \frac{\nu}{U_e}\frac{R_e^{1.5}}{3\Lambda_e} - \frac{\nu R_e^{0.5} R_{x,e}}{U_e \Lambda_e} - \frac{2\nu^2}{U_e^2 \Lambda_e^2} R_{x,e} \tag{33}$$

$$\frac{dR_{y,e}}{d\xi} = \frac{\nu R_e^{1.5}}{3U_e\Lambda_e} - \frac{\nu}{U_e}\frac{R_e^{0.5}R_{y,e}}{\Lambda_e} - \frac{2\nu^2}{U_e^2\Lambda_e^2}R_{y,e} \qquad (34)$$

and,

$$\frac{dR_{z,e}}{d\xi} = -\frac{2R_{z,e}}{U_e}\frac{dU_e}{d\xi} + \frac{\nu R_e^{1.5}}{3U_e\Lambda_e} - \frac{\nu R_e^{0.5}}{U_e\Lambda_e}R_{z,e} - \frac{2\nu^2}{U_e^2\Lambda_e^2}R_{z,e} \qquad (35)$$

The above equations are solved for the Reynolds normal stresses. The sum of the Reynolds normal stresses R_e should be consistent with the turbulence kinetic energy obtained from Eqs. (30) and (31) (see Appendix A).

The previous analysis of the initial conditions for Region 3 defines the Reynolds normal stresses at (ξ_2,η_2). These initial conditions are used to integrate Eqs. (33) to (35) along the downstream direction. The Fourth Order Runge-Kutta numerical method is used for the integration. The turbulence kinetic energy obtained previously from Eqs. (30) and (31) is used to evaluate the derivatives. The integration step is adjusted until the turbulence kinetic energy $(R_{x,e} + R_{y,e} + R_{z,e})U_e^2/2$ satisfactorily converges to the corresponding value predicted by the k and ε equations. The corresponding Reynolds normal stresses are the boundary conditions at the boundary layer edge.

Finally, the following conditions are also imposed:

1. at the surface $\eta = 0$,

$$F = 0, \quad H = T_w/T_e, \quad R_x = 0, \quad R_y = 0,$$

$$R_z = 0, \quad S = 0, \quad \text{and} \quad \theta = 0$$

2. at the boundary layer edge $\eta = \eta_2$,

$$F_e = 1, \quad H_e = 1, \quad S_e = c_5(R_{x,e}R_{y,e})^{0.5},$$

$$\text{and} \quad \theta = 0$$

A numerical computational procedure to calculate the boundary layer flow field described by Eqs. (11) to (18) was developed in a previous study (12). This existing numerical computational procedure is used to calculate the turbulence correlations and the mean flow properties in Flow Region 3.

RESULTS AND COMPARISON WITH EXPERIMENT

In order to verify the above theoretical analysis, a numerical computation was performed to compare the analysis with existing experimental measurements. A set of experimental data on the effect of freestream turbulence on heat transfer from heated cylinders placed normal to airstream was reported in Ref. 1. The two point turbulence longitudinal correlations in the freestream were also measured in that experiment. These data are used to determine the turbulence longitudinal microlength scale which is required to start the present numerical calculations. Thus, the test conditions of this reference were used as input to the present numerical computational procedures. The turbulence longitudinal microlength scales are obtained by curve-fitting the experimental data using Eq. (3). Based on the freestream mean velocity, the freestream turbulence intensity, and the turbulence longitudinal microlength scale, the turbulence kinetic energy, the turbulence double correlations, and the mean flow properties within the stagnation flow field are computed. The surface heat transfer rate is also calculated from the mean temperature distribution. In the following sections these numerical results are described and are compared with the experiment of Ref. 1.

Turbulence

To show the variation of the turbulence kinetic energy along the stagnation point streamline, some analytical results are plotted in Fig. 3. Except for the lowest turbulence case, the turbulence kinetic energy increases within the inviscid flow region in the direction toward the surface and reaches a maximum value at the boundary layer edge. The turbulence kinetic energy then decreases continuously and vanishes at the cylinder surface. This turbulence kinetic energy variation is similiar to the results in Ref. 10. However, the present analysis also predicts a reduction in the turbulence kinetic energy along the stagnation point streamline when the freestream turbulence intensity and Reynolds number are small, (Tu = 0.013 and $Re = 1.90\times10^5$). With constant Reynolds number, increasing the freestream turbulence intensity also increases the turbulence kinetic energy at the boundary layer edge ($\eta \approx 5$).

Examples of the Reynolds normal stress profiles within the boundary layer at the stagnation point are shown in Fig. 4. These results are for the cases with $Re = 2.5\times10^5$ and Tu = 0.017 and 0.028. The Reynolds normal stresses decrease continuously from the boundary layer edge in a direction normal to the surface. The R_y value was predicted to be the largest for a small region very near the surface. These Reynolds normal stress profiles differ significantly from those of a flat plate turbulent boundary layer (18) where the largest Reynolds normal stress was found in the x-direction.

Analytical predictions of the mean velocity component, $F = U/U_e$ within the boundary layer near the stagnation point are shown in Fig. 5. These profiles are compared with the mean velocity profile of the theoretical laminar boundary layer. The comparison shows that increasing the freestream turbulence increases the velocity near the surface and decreases the velocity near the boundary layer edge. Existing measurements (19) of this velocity component F with $Re = 2.5\times10^5$ and Tu $\approx$ 0.05 are also plotted in this figure. The analysis agrees with the measurements.

Example of the computational results of the turbulence kinetic energy and the Reynolds normal stresses along the boundary layer edge are shown in Fig. 6. In this figure, the turbulence quantities are nondimensionalized with the corresponding values at (ξ_2,η_2). The turbulence kinetic energy increases continuously along the downstream direction. Large increase in the turbulence kinetic energy is found for the case with small freestream Reynolds number and turbulence intensity. The Reynolds normal stress components, u_e^2 and v_e^2, increase monotonically at the downstream locations. However, the w_e^2 component shows a reduction near the stagnation point. The effect of the freestream turbulence longitudinal microlength scale on the Reynolds normal stresses along the boundary layer edge is shown in Fig. 7. Increasing the turbulence longitudinal microlength scale is shown to decrease the value of $u_e^2/u_{0,e}^2$ and increases the value of $w_e^2/w_{0,e}^2$ along the boundary layer edge. No significant difference in the value of $v_e^2/v_{0,e}^2$ is calculated.

Surface Heat Transfer

The present analytical results of the surface heat transfer is defined in terms of the Nusselt number;

$$Nu = -D \left(\frac{\partial T}{\partial y}\right)_{y=0} \Big/ (T_w - T_F) \qquad (36)$$

The mean temperature gradient $(\partial T/\partial y)_{y=0}$ at the surface is calculated numerically from the mean temperature profile, which in turn, was obtained previously from the solution of the boundary layer flow.

The analytical results for the stagnation point surface heat transfer rate over a range of the freestream Reynolds number and the turbulence intensity are compared with experimental data (1) and existing correlations (1,2) in Fig. 8. The surface heat transfer rate is expressed in the form of the Froessling number ($NuxRe^{-0.5}$). Linear variation in the turbulence longitudinal microlength scale as function of the freestream Reynolds number is also assumed in the present calculation. With constant freestream turbulence intensity, the longitudinal turbulence microlength scales within ±10 percent of the values at $Re = 2.5x10^5$ were used in the numerical computation for a range of $1.5<Rex10^{-5}<3.0$. Including the effect of the freestream turbulence microlength scale, the present analysis calculates a larger stagnation point surface heat transfer rate than is indicated by the correlations in Refs. 1 and 2.

Examples of the computational results of the turbulence double correlation $-\overline{vt}/U_eT_e$ within the boundary layer at the stagnation point are shown in Fig. 9. The maximum turbulence correlation occurs near the surface. Increasing the freestream turbulence intensity also increases the turbulence correlation $\overline{vt}$. Together with the characteristics of the Reynolds normal stress component R_y as shown in Fig. 4, Eqs. (13) and (18) predict a high heat transfer rate at the surface. It is postulated that the freestream turbulence penetrates into the near surface flow region and induces large turbulence correlation $\overline{vt}$. Thus, a surface heat transfer rate larger than that of a laminar flow occurs.

Some analytical results of the surface heat transfer rate within a small distance from the stagnation point are plotted in Fig. 10 in terms of Froessling number. Approximately constant Froessling number is calculated only for the case with Tu = 0.013. For Tu = 0.017 and 0.028, the analytical results show a reduction in the Froessling number near the stagnation point. With high freestream turbulence intensity, a large turbulence dissipation rate may occur near the stagnation point (Eq. (2)). This turbulence dissipation rate reduces the rate of the increase in the turbulence kinetic energy. This rate of increase in K_e may not be sufficient to induce a constant surface heat transfer rate.

To investigate the effect of the turbulence longitudinal microlength scale on the surface heat transfer rate, the analytical results of the turbulence kinetic energy and the Froessling number for the cases of $\lambda_F/D = 0.0053$ and 0.0079 with $Re = 2.5x10^5$ and Tu = 0.028 are compared in Fig. 11. With $\lambda_F/D = 0.0079$, the present analysis computes the experimental data in Ref. 1. A lower level of the turbulence kinetic energy and a smaller Froessling number are also predicted for the case with small freestream turbulence longitudinal microlength scale. These computational results also show a reduction in the Froessling number near the stagnation point.

In this study, the approximation, $S_e = C_5(R_{x,e}R_{y,e})^{0.5}$, is used along the boundary layer edge. This approximation is similar to the the correlation observed from the flat plate turbulent boundary layer study (18). The constant $c_5 = 0.001$ is found to give the best computational results in the present analysis. In an earlier study (12), a different value of $c_5 = 0.0001$ was used because the boundary layer edge location and the corresponding turbulence kinetic energy (or the Reynolds normal stresses) were not analyzed theoretically. If one uses the small value of c_5, then a small (nonzero) $\overline{uv}$ is imposed along the boundary layer edge. This approximation is different from the k-ε two-equation turbulence modeling, which requires $\overline{uv}$ to be zero for the external inviscid flow field in this study. However, the requirement of $\overline{uv} = 0.$ is itself an assumption.

The assumption $-\overline{vt} = 0$ is also imposed at the boundary layer edge. Intuitively, the turbulence transport equations can also be used to study the variation of the turbulence double correlation $\overline{vt}$ within the external inviscid flow region. If $\overline{vt}$ is nonzero in the external flow field, then different $\overline{vt}$ may occur within the boundary layer flow region and the present analysis will predict different stagnation flow surface heat transfer rate. If this is true, it might resolve the different level of the stagnation flow surface heat transfer rate reported in various experiments. Although, the task requires the $\overline{vt}$ boundary condition within the freestream, the effect of the freestream temperature fluctuation on the surface heat transfer rate of the stagnation flow can be studied using the present analysis.

CONCLUSIONS

Theoretical analysis was formulated to model the effect of the freestream turbulence on the surface heat transfer of a stagnation flow region. The flow field of interest is around the forward stagnation point of a circular cylinder in a turbulent flow. The k-ε two-equation turbulence modeling was used to analyze the turbulence kinetic energy within external inviscid flow. The time-averaged turbulence transport equations were employed to predict the turbulence double correlations within the boundary layer. Based on the boundary layer edge conditions of the turbulence kinetic energy, the transport equations of the mean flow and turbulence are solved numerically for the turbulence double correlations, the mean velocity and the mean temperature.

The present analytical results show that, depending on the freestream turbulence properties, different levels of turbulence kinetic energy occur along the boundary layer edge. These different levels of turbulence kinetic energy induce different surface heat transfer rates. Increasing the freestream turbulence intensity or the turbulence longitudinal microlength scale also increases the stagnation region surface heat transfer rate. It is postulated that the freestream turbulence penetrates into the boundary layer and induces high surface heat transfer rate.

The analysis presents a procedure to calculate the stagnation point surface heat transfer rate as functions of the freestream turbulence intensity, turbulence longitudinal microlength scale and Reynolds number. Due to limited data on the turbulence longitudinal microlength scale, this analysis was verified only for some cases with Reynolds number of the order of 10^5 and the freestream turbulence intensity of less than 5 percent. Considering the freestream turbulence longitudinal microlength scale, this analysis predicts a higher stagnation point surface heat transfer rate than was obtained from the existing correlations

relating the freestream turbulence intensity, Reynolds number and the surface heat transfer rate.

APPENDIX A

The turbulence kinetic energy and its dissipation rate along the stagnation point streamline and the boundary layer edge are calculated respectively from Eqs. (6) and (7), and Eqs. (30) and (31). Finite difference method is used to solve these equations for the K and E distributions which satisfy the boundary conditions.

The dimensionless Eqs. (6) and (7) can be written as

$$A_{\eta 1}\frac{dG}{d\eta} = A_{\eta 2}G + A_{\eta 3}\frac{d}{d\eta}\left(A_{\eta 4}\frac{dG}{d\eta}\right) + A_{\eta 5} \qquad (A1)$$

with G = K or E

Similarly, Eqs. (30) and (31) can also be written as

$$A_{\xi 1}\frac{dG}{d\xi} = A_{\xi 2}G + A_{\xi 3}\frac{d}{d\xi}\left(A_{\xi 4}\frac{dG}{d\xi}\right) + A_{\xi 5} \qquad (A2)$$

with G = K or E.

In the above equations, $A_{\xi i}$ and $A_{\eta i}$ may be constant, or the functions of the turbulence properties, or coordinates ξ and η.

A similar finite difference scheme is used to convert Eqs. (A1) and (A2) into finite difference forms. The derivatives at each grid point m are approximated by central finite difference. A finite difference equation

$$B_1 G_{m+1} + B_2 G_m + B_3 G_{m-1} = B_4 \qquad (A3)$$

is found at each grid point m. The coefficients B_i (i = 1 to 4) are functions of the various coefficients $A_{\xi 1}$ or $A_{\xi i}$, and the grid size at the grid points m+1, m, m-1.

Applying the previous mathematical manipulation at every grid point within the interval $\eta 1 \geq \eta \geq \eta 2$ or $\xi 2 \geq \xi \geq \xi 3$ results in a set of finite difference equations for Eq. (A1) or Eq. (A2). The boundary conditions of G are specified at $\eta 1$ and $\eta 2$ (or $\xi 2$ and $\xi 3$). This set of equations are solved for the G values at each grid point m. The grid size within the computational interval is generated using the model in Ref. 20. Two hundred to four hundred grid points are used in the numerical computation.

Equations (8) to (10) describe the boundary conditions at $\eta = \eta 1$ and $\eta 2$. However, the value of $\eta 2$ is not yet defined. Therefore, an arbitrary value is assigned to $\eta 2$ to start the numerical calculation. The existing analysis (10) indicates that $\eta 2$ is approximately equal to 5.0. Linear variations in K and E are first assumed. The coefficients of the finite difference equations are evaluated using these K and E distributions. Thus, two sets of linear algebraic equations are obtained to relate K and E at the grid points. Since K and E are prescribed at $\eta 1$ and $\eta 2$, these equations are solved to update the K and E distributions using the method of successive substitution. The above procedures are repeated until K and E converge at each grid point. The boundary values of K and E at $\eta 2$ are adjusted to assure that K and E profiles satisfy the boundary conditions at $\eta 1$ and $\eta 2$.

The convergence in K and E is sensitive to their assumed values at the start of the computations. Based on the k-ε two-equation turbulence modeling, Strahle (11) developed analytical links between the turbulence properties k and ε at the stagnation point and in the freestream. Neglecting the diffusion terms and using the same value for the empirical constants c_1 and c_2, ($c_1 = c_2 = 1.90$), these analytical links can be written in nondimensionalized forms as

$$k_2 = \left(\frac{2.4\ V_F}{D\varepsilon_F}\right)^{1.111} k_F^{2.111} \qquad (A4)$$

and

$$E_2 = (0.6\ K_F)^{2.111} E_F^{-1/1.111} \qquad (A5)$$

With the isotropic assumptions, Eq. (2), the approximate boundary conditions for K and E at $\eta 2$ are calculated from the previous relations. These K and E values are used to start the numerical computations.

The previously mentioned numerical calculation provides the conditions of K and E at $\xi 2$. Based on these conditions, the K and E along the boundary layer edge are also calculated from the sets of finite difference equations corresponding to Eq. (A2). The computational domain, $\xi 2 \leq \xi \leq \xi 3$ is limited to a small region near the stagnation point, ($0.04^\circ \leq \varphi \leq 15.0^\circ$).

First, K and E at $\xi 3$ location are estimated and linear distributions in K and E between $\xi 2$ and $\xi 3$ are assumed. The coefficients of the finite difference equations are calculated using the assumed K and E distributions. Two sets of linear algebraic equations relating the K and E at the grid points are obtained. These algebraic equations are solved with the method of successive substitution to update the K and E distributions. This iterative computational procedure is repeated until K and E converge at each grid point. The values of K and E at $\xi 3$ are also adjusted in each iteration to facilitate the convergence in the numerical computations.

REFERENCES

1. Lowery, G.W., and Vachon, R.I., 1975, "The Effect of Turbulence on Heat Transfer from Heated Cylinders," International Journal of Heat and Mass Transfer, Vol. 18, No. 11, pp. 1229-1242.

2. Smith, M.C., and Kuethe, A.M., 1966, "Effects of Turbulence on Laminar Skin Friction and Heat Transfer," Physics of Fluids, Vol. 9, No. 12, pp. 2337-2344.

3. Gorla, R.S.R., 1983, "Combined Influence of Unsteady Free Stream Velocity and Free Stream Turbulence on Stagnation Point Heat Transfer," ASME Paper 83-GTJ-17.

4. Kestin, J., and Wood, R.T., 1971, "The Influence of Turbulence on Mass Transfer from Cylinders," Journal of Heat Transfer, Vol. 93, No. 4, pp. 321-327.

5. Sutera, S.P., Maeder, P.F., and Kestin, J., 1963, "On the Sensitivity of Heat Transfer in the Stagnation-Point Boundary Layer to Free-Stream Vorticity," Journal of Fluid Mechanics, Vol. 16, Pt. 4, pp. 497-520.

6. Sutera, S.P., 1965, "Vorticity Amplification in Stagnation-Point Flow and Its Effect on Heat Transfer," Journal of Fluid Mechanics, Vol. 21, Pt. 3, pp. 513-534.

7. VanFossen, G.J., Jr., and Simoneau, R.J., 1985, "Preliminary Results of a Study of the Relationship Between Free Stream Turbulence and Stagnation Region Heat Transfer," ASME Paper 85-GT-84. (NASA TM-86884).

8. O'Brien, J.E., and Van Fosen, G.J., Jr., 1985, "The Influence of Jet-Grid Turbulence on Heat Transfer from the Stagnation Region of a Cylinder in Crossflow," ASME Paper 85-HT-58. (NASA TM-87011).

9. Hijikata, K., Yoshida, H., and Mori, Y., 1982, "Theoretical and Experimental Study of Turbulence Effects on Heat Transfer Around the Stagnation Point of a Cylinder," Heat Transfer 1982, Vol. 3, U. Grigull et al., eds., Hemisphere Publishing, Washington, D.C., pp. 165-170.

10. Traci, R.M., and Wilcox, D.C., 1975, "Freestream Turbulence Effects on Stagnation Point Heat Transfer," AIAA Journal, Vol. 13, No. 7, pp. 890-896.

11. Strahle, W.C., 1985, "Stagnation Point Flows with Freestream Turbulence - The Matching Condition," AIAA Journal, Vol. 23, No. 11, pp. 1822-1824.

12. Wang, C.R., 1984, "Turbulence and Surface Heat Transfer Near the Stagnation Point of a Circular Cylinder in Turbulent Flow," ASME Paper 84-WA/HT-73. (NASA TM-83732).

13. Hinze, J.O., 1959, Turbulence, McGraw-Hill, New York.

14. Launder, B.E., and Spalding, D.B., 1974, "The Numerical Computation of Turbulent Flows," Computer Methods in Applied Mechanics and Engineering, Vol. 3, No. 2, pp. 269-289.

15. Donaldson, C. duP., Sullivan, R.D., and Rosenbaum, H., 1972, "A Theoretical Study of the Generation of Atmospheric-Clear Air Turbulence," AIAA Journal, Vol. 10, No. 2, pp. 162-170.

16. Donaldson, C. duP., 1969, "A Computer Study of an Analytical Model of Boundary-Layer Transition," AIAA Journal, Vol. 7, No. 2, pp. 271-278.

17. Wang, C.R., and Yeh, F.C., 1987, "Application of Turbulence Modeling to Predict the Surface Heat Transfer in the Stagnation Flow Region of a Circular Cylinder," NASA Technical Paper, to be published.

18. Schilchting, H., 1960, Boundary Layer Theory, 4th ed., McGraw-Hill, New York.

19. Kestin, J., and Richardson, P.D., 1969, "The Effects of Free-Stream Turbulence and of Sound Upon Heat Transfer," ARL 69-0062, Wright-Patterson AFB, OH. (Avail. NTIS, AD-691497).

20. Andre, P., Creff, R., and Batina, J., 1986, "Numerical Study in Heat Transfer for a Turbulent Pulsed Ducted Flow," Numerical Heat Transfer, Vol. 9, No. 2, pp. 201-215.

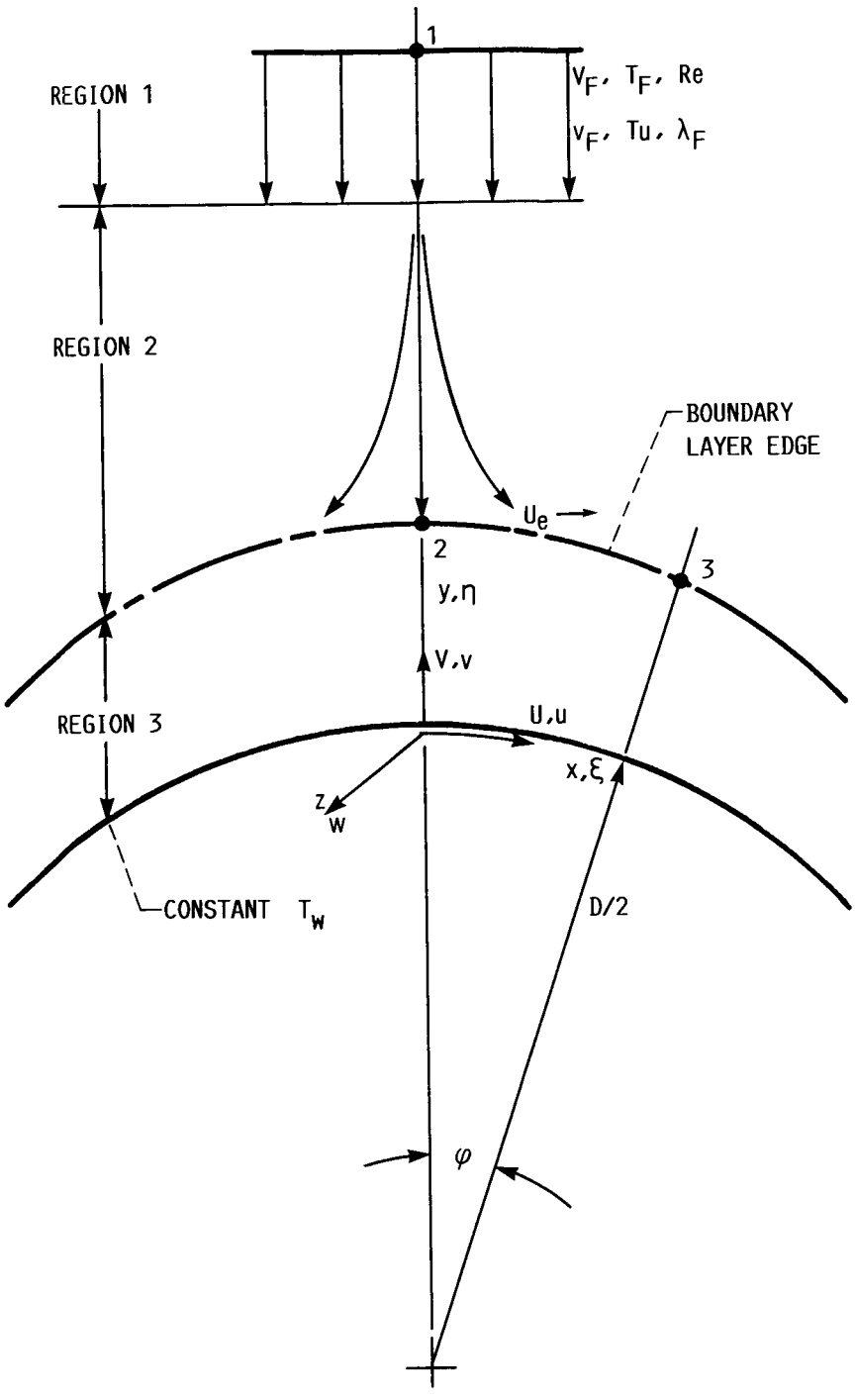

FIGURE 1. - A SCHEMATIC OF FLOW FIELD OF INTEREST.

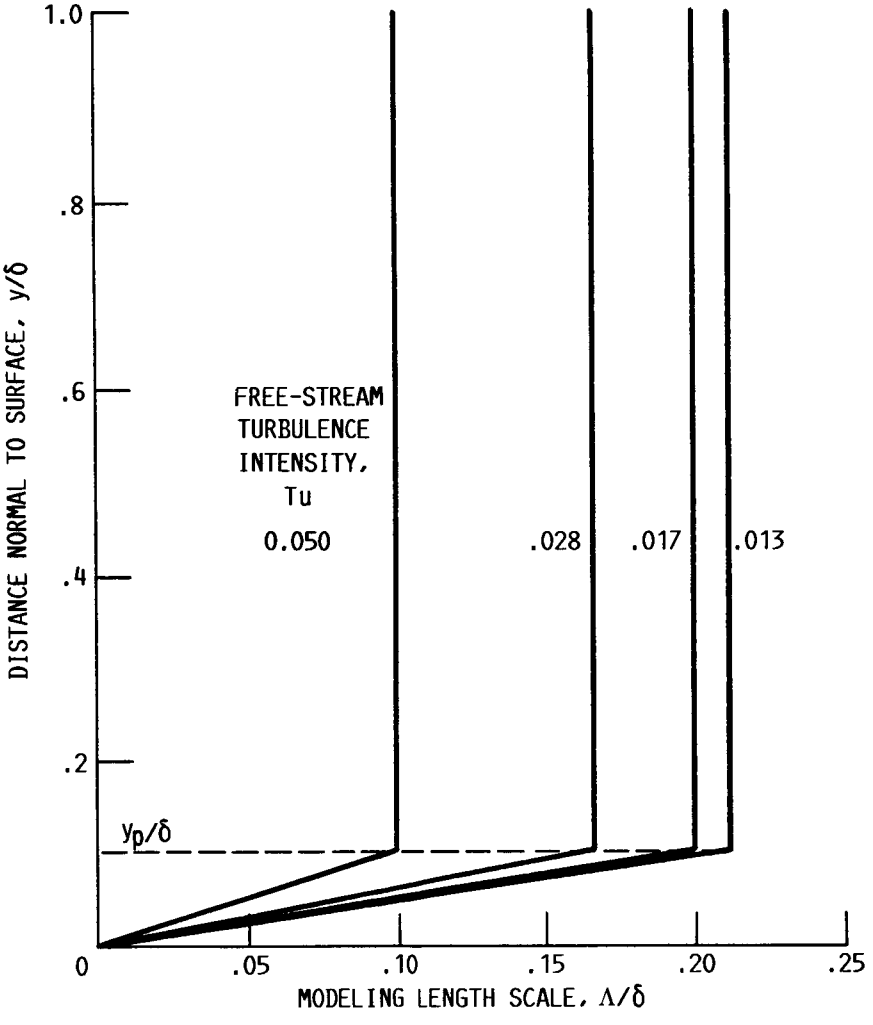

FIGURE 2. - MODELING LENGTH SCALE OF THE TURBULENCE CLOSURE ASSUMPTIONS.

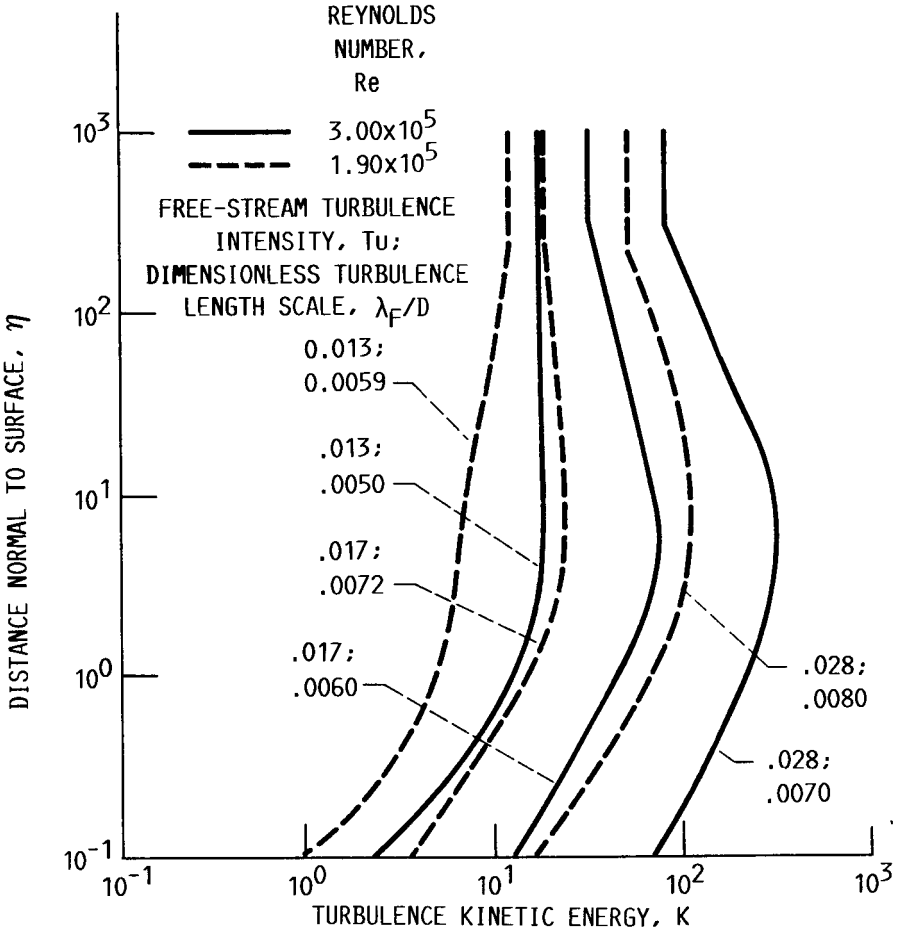

FIGURE 3. - TURBULENCE KINETIC ENERGY ALONG THE STAGNATION STREAMLINE.

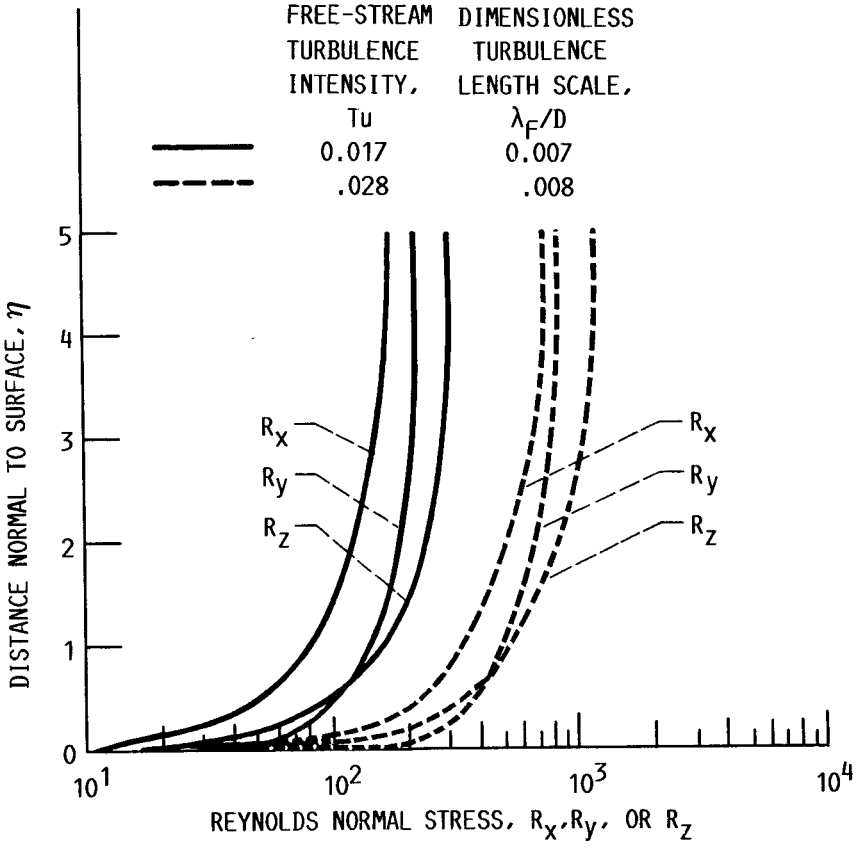

FIGURE 4. - REYNOLDS NORMAL STRESS PROFILES WITHIN THE STAGNATION POINT BOUNDARY LAYER, Re = 2.5×10^5.

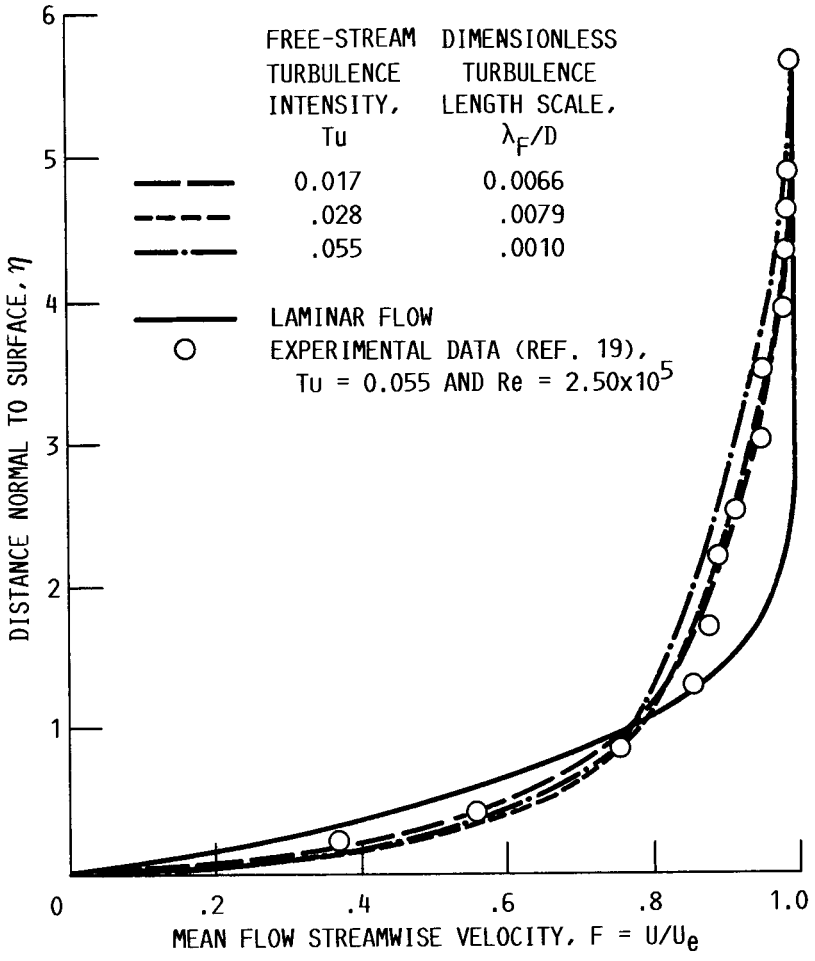

FIGURE 5. - MEAN FLOW STREAMWISE VELOCITY COMPONENT WITHIN THE STAGNATION POINT BOUNDARY LAYER, $Re = 2.5 \times 10^5$.

	REYNOLDS NUMBER, Re	DIMENSIONLESS TURBULENCE LENGTH SCALE, λ_F/D	DIMENSIONLESS FREE-STREAM TURBULENCE KINETIC ENERGY, K_F	DIMENSIONLESS FREE-STREAM TURBULENCE DISSIPATION RATE, E_F	DIMENSIONLESS TURBULENCE KINETIC ENERGY, $K_{o,e}$	DIMENSIONLESS TURBULENCE DISSIPATION RATE, $E_{o,e}$
———	1.96×10^5	0.0053	12.27	11.45	7.51	3.79
- - - -	3.00×10^5	.0053	19.06	11.45	19.03	11.42

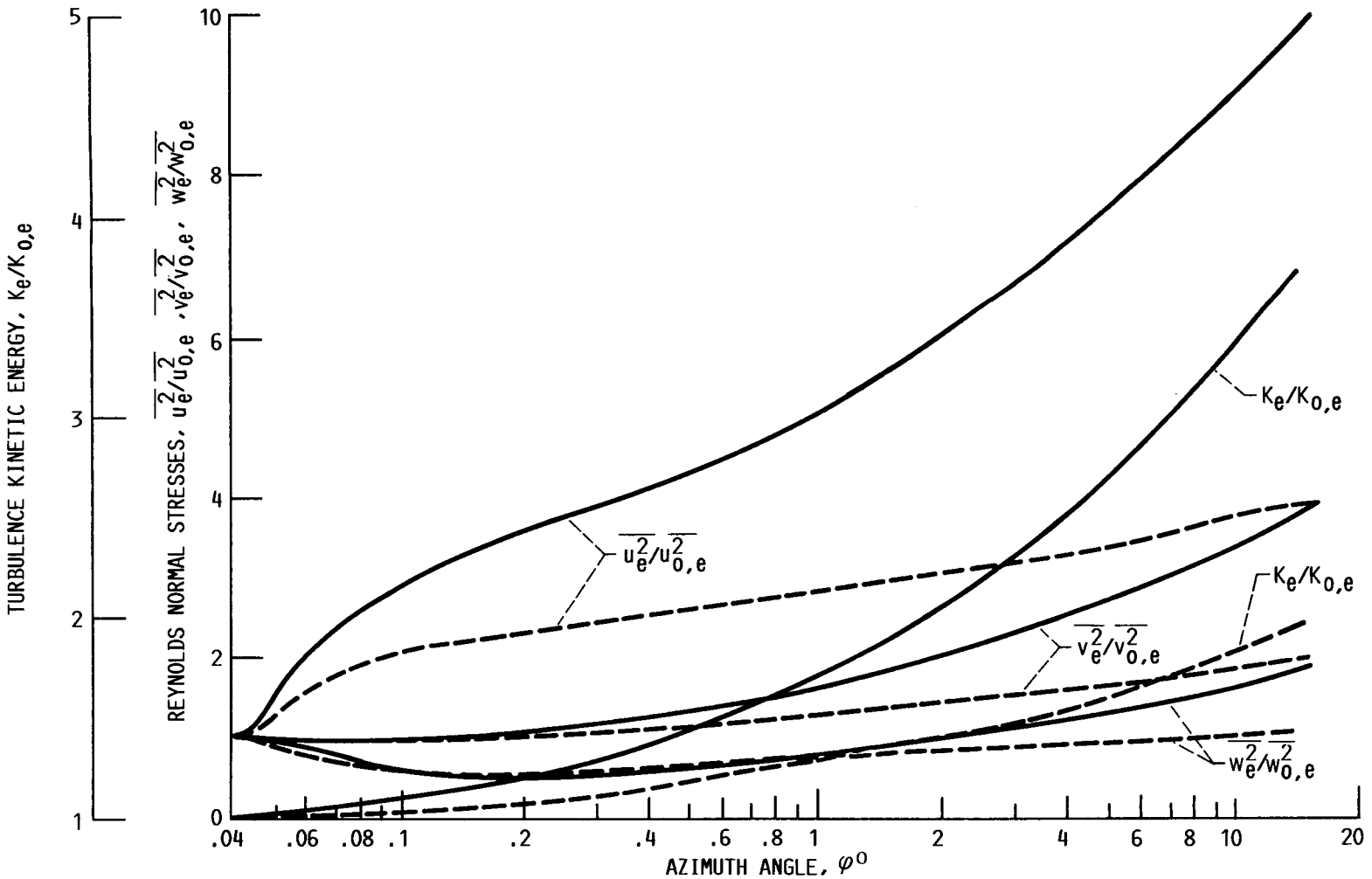

FIGURE 6. - BOUNDARY LAYER EDGE TURBULENCE KINETIC ENERGY AND CORRESPONDING FROESSLING NUMBER, Tu = 0.013.

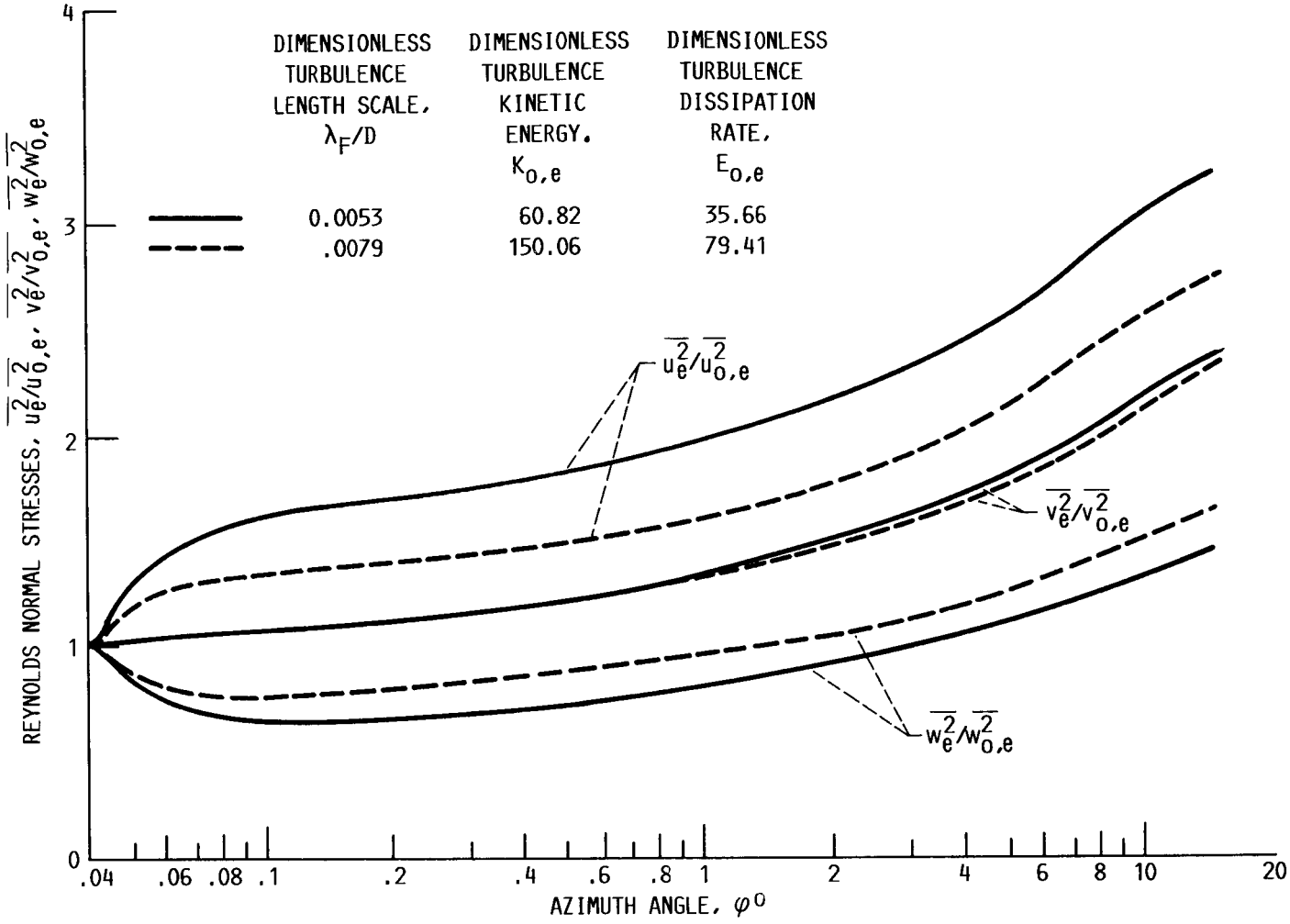

FIGURE 7. - EFFECT OF THE TURBULENCE LONGITUDINAL MICROLENGTH SCALE ON THE REYNOLDS NORMAL STRESSES ALONG THE BOUNDARY LAYER EDGE, Re = 2.5×10^5 AND Tu = 0.028.

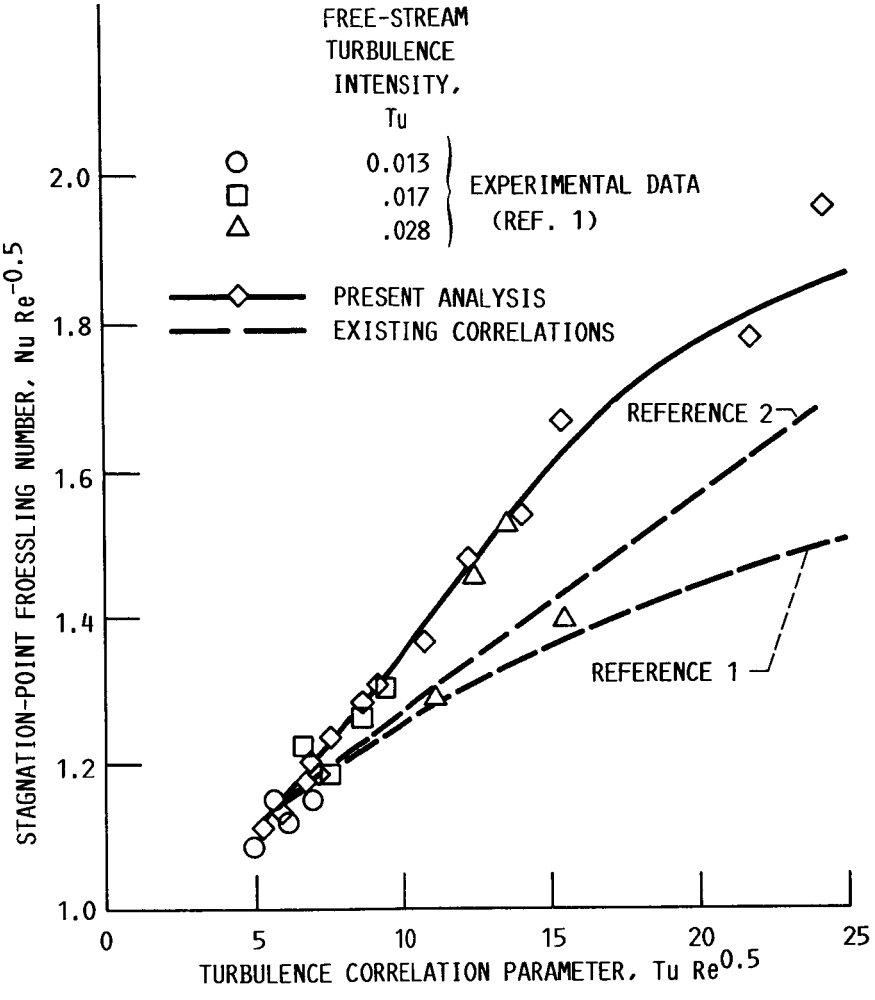

FIGURE 8. - COMPARISON OF THE STAGNATION POINT FROESSLING NUMBER BETWEEN THE ANALYSIS AND EXPERIMENTAL CORRELATIONS.

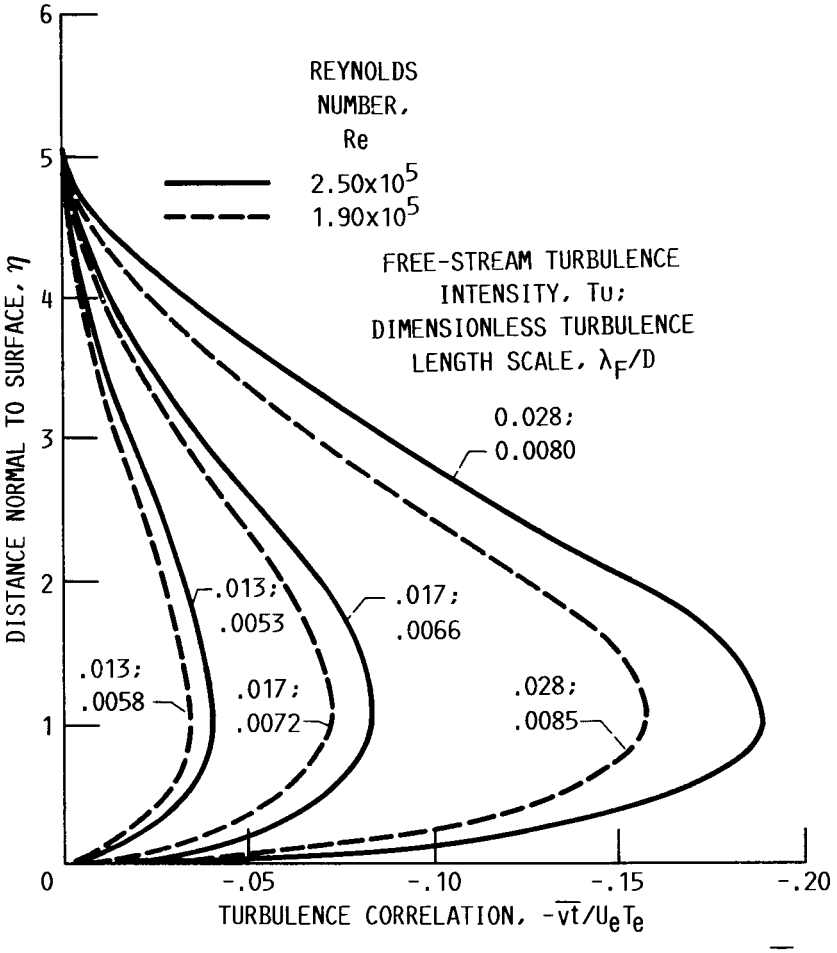

FIGURE 9. - PROFILES OF THE TURBULENCE CORRELATION $\overline{vt}$ WITHIN THE STAGNATION POINT BOUNDARY LAYER.

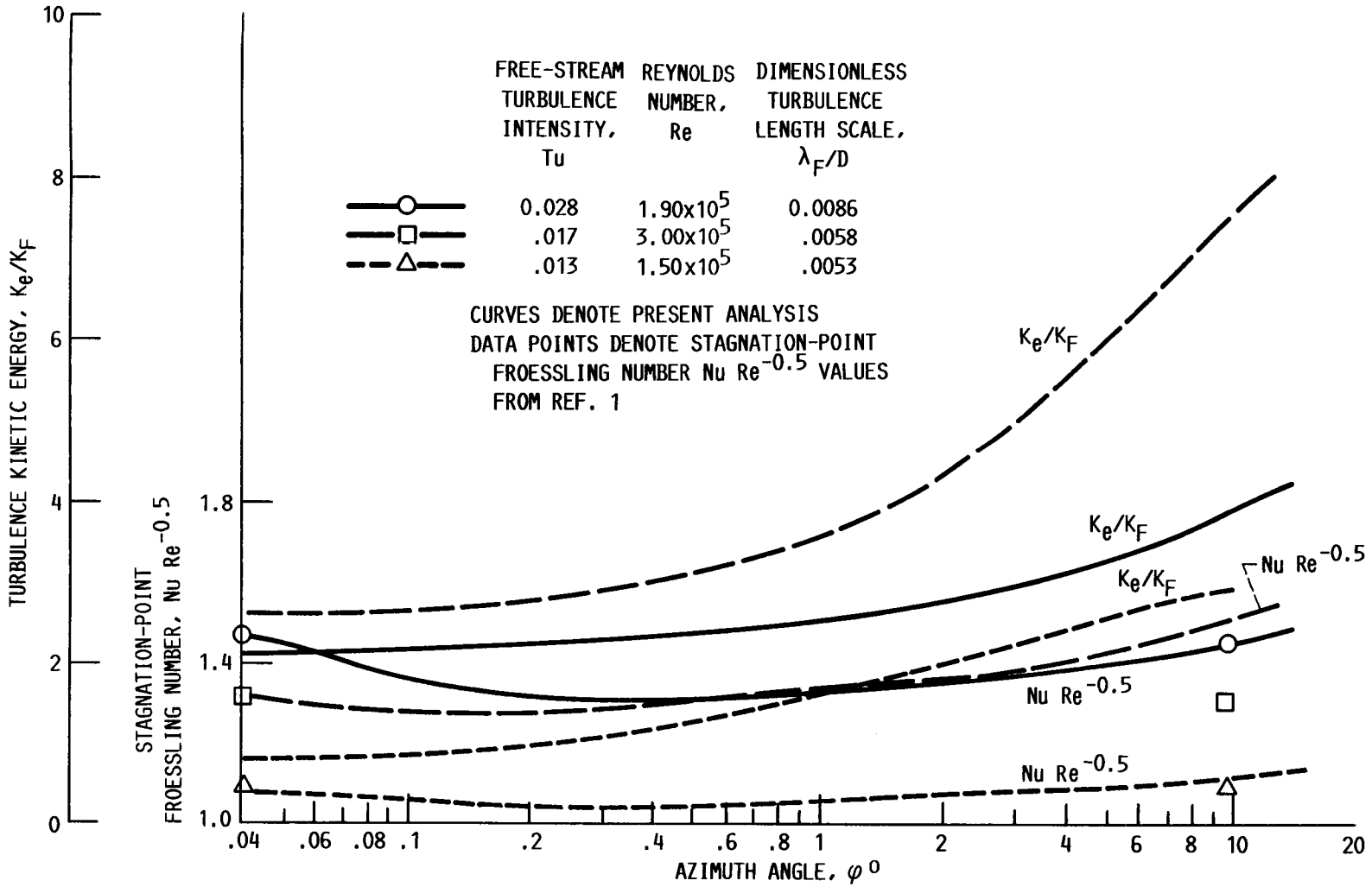

FIGURE 10. - TURBULENCE KINETIC ENERGY AND REYNOLDS NORMAL STRESSES ALONG THE BOUNDARY LAYER EDGE.

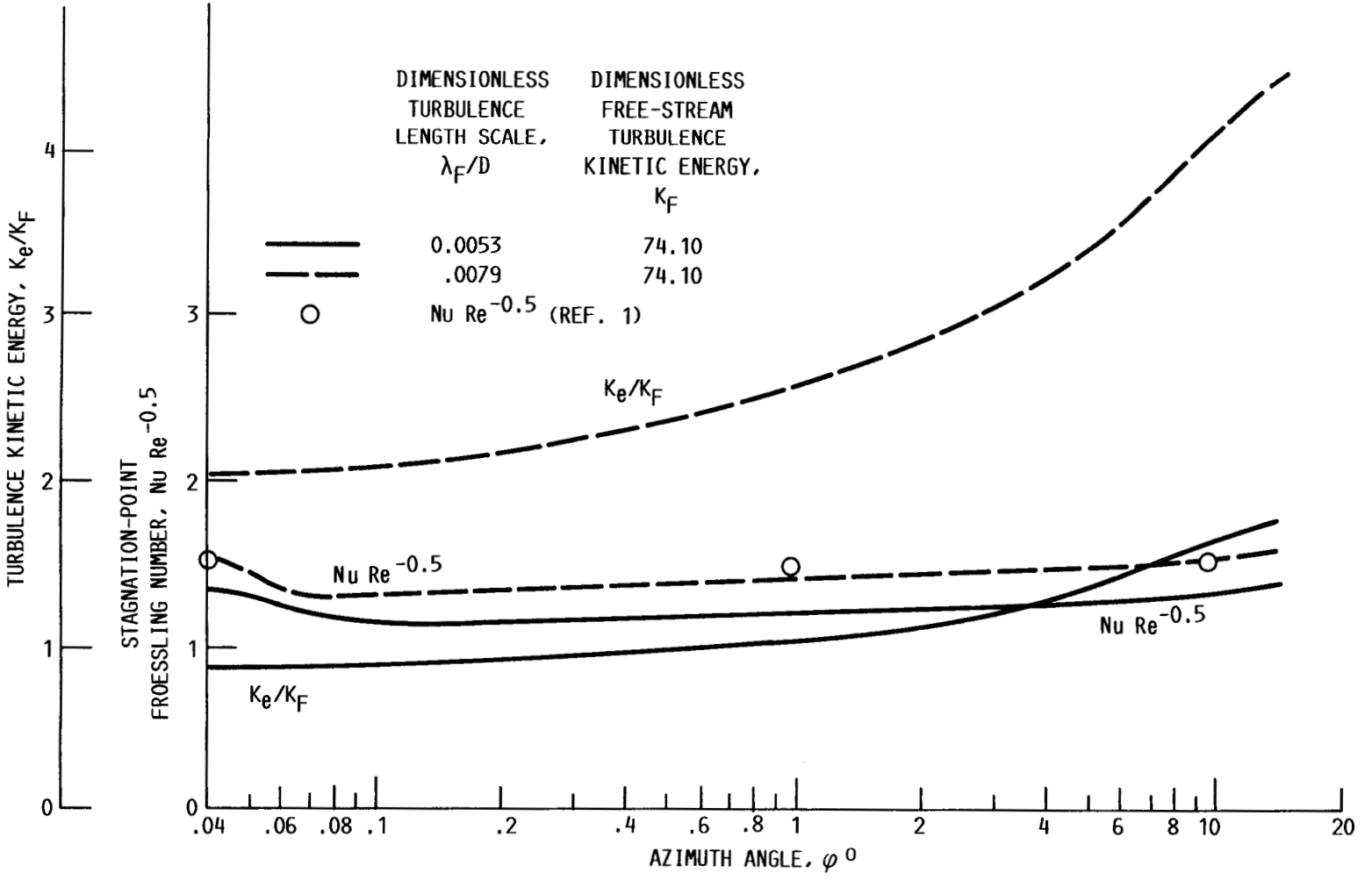

FIGURE 11. - EFFECT OF THE TURBULENCE LONGITUDINAL MICROLENGTH SCALE ON THE TURBULENCE KINETIC ENERGY AT THE BOUNDARY LAYER EDGE AND FROESSLING NUMBER, Re = 2.5×10^5 AND Tu = 0.028.

NASA
National Aeronautics and Space Administration

Report Documentation Page

1. Report No.	2. Government Accession No.	3. Recipient's Catalog No.
NASA TM-100132		

4. Title and Subtitle

Turbulence Modeling and Surface Heat Transfer in a Stagnation Flow Region

5. Report Date

6. Performing Organization Code

505-62-21

7. Author(s)

Chi R. Wang and Frederick C. Yeh

8. Performing Organization Report No.

E-3682

10. Work Unit No.

9. Performing Organization Name and Address

National Aeronautics and Space Administration
Lewis Research Center
Cleveland, Ohio 44135

11. Contract or Grant No.

13. Type of Report and Period Covered

Technical Memorandum

12. Sponsoring Agency Name and Address

National Aeronautics and Space Administration
Washington, D.C. 20546

14. Sponsoring Agency Code

15. Supplementary Notes

Prepared for the 1987 Winter Annual Meeting of the American Society of Mechanical Engineers, Boston, Massachusetts, December 13-18, 1987.

16. Abstract

Analysis for the turbulent flow field and the effect of freestream turbulence on the surface heat transfer rate of a stagnation flow are presented. The emphasis is on the modeling of turbulence and its augmentation of surface heat transfer rate. The flow field considered is the region near the forward stagnation point of a circular cylinder in a uniform turbulent mean flow. The freestream is steady and incompressible with a Reynolds number of the order of 10^5 and turbulence intensity of <5 percent. The flow field is divided into three regions: (1) a uniform freestream region where the turbulence is homogeneous and isotropic; (2) an external inviscid flow region where the turbulence is distorted by the variation of the mean velocity; and (3) an anisotropic turbulent boundary layer flow region. The turbulence modeling techniques are the k-ε two-equation model in the external flow and the time-averaged turbulence transport equation in the boundary layer. The turbulence double correlations, the mean velocity, and the mean temperature within the boundary layer are solved numerically from the transport equations. The surface heat transfer rate is calculated as functions of the freestream turbulence longitudinal microlength scale, turbulence intensity, and Reynolds number.

17. Key Words (Suggested by Author(s))	18. Distribution Statement
Heat transfer Boundary layer Turbulence	Unclassified - unlimited STAR Category 34

19. Security Classif. (of this report)	20. Security Classif. (of this page)	21. No of pages	22. Price*
Unclassified	Unclassified	21	A02

*For sale by the National Technical Information Service, Springfield, Virginia 22161